

# The impact of model grid resolution on Gulf Stream dynamics in idealised simulations

---

**Topić, Roko**

**Undergraduate thesis / Završni rad**

**2021**

*Degree Grantor / Ustanova koja je dodijelila akademski / stručni stupanj:* **University of Split, University of Split, Faculty of science / Sveučilište u Splitu, Prirodoslovno-matematički fakultet**

*Permanent link / Trajna poveznica:* <https://urn.nsk.hr/urn:nbn:hr:166:569248>

*Rights / Prava:* [Attribution-NonCommercial-NoDerivatives 4.0 International/Imenovanje-Nekomercijalno-Bez prerada 4.0 međunarodna](#)

*Download date / Datum preuzimanja:* **2024-11-19**

*Repository / Repozitorij:*

[Repository of Faculty of Science](#)



University of Split  
Faculty of Science

**The impact of model grid resolution on Gulf  
Stream dynamics in idealised simulations**

Bachelor thesis

Roko Topić

Split, studeni 2021.

## Acknowledgements

First of all, I thank prof. dr. sc. Joakim Kjelsson for his contribution to this thesis. Him and prof. dr. sc. Torge Martin provided the guidance and expertise necessary for this thesis to obtain its current form.

I would also like to thank my professors and colleagues at Physics department at my home University of Split.

## Temeljna dokumentacijska kartica

Sveučilište u Splitu  
Prirodoslovno – matematički fakultet  
Odjel za fiziku  
Ruđera Boškovića 33, 21000 Split, Hrvatska

Završni rad

### Utjecaj rezolucije modela na dinamiku Golfske struje u idealiziranim simulacijama

Roko Topić

Sveučilišni preddiplomski studij Fizika

#### Sažetak:

Golfska struja jedna je od najvećih i povijesno-geografski najznačajnijih morskih struja. Nastaje kao posljedica termodinamičkih i mehaničkih procesa u atmosferi i oceanu te pod utjecajem planetarne rotacije poprima svoj konačni oblik. Izmjena topline između sjevernog dijela Atlantskog oceana i nadkrovnog atmosferskog sloja ima poseban značaj za klimatski profil Europe i Sjeverne Amerike. U ovom radu, cilj je usporediti različite simulacije sjevernoatlantskog oceana pomoću NEMO (Nucleus for European Modelling of the Ocean) alata za modeliranje oceana koji slijedi skup jednadžbi koje određuju dinamiku mora - primitivne jednadžbe. Idealizirani model, usporediv sa sjevernoatlantskim bazenom, s rezolucijskom preciznošću od  $1/2^\circ$ ,  $1/4^\circ$ ,  $1/10^\circ$  i  $1/20^\circ$  je korišten u svrhu predočavanja utjecaja zadanih modelacijskih parametara i odabrane rezolucije na ponašanje morske struje. Analiziranjem kinetičke energije i pozicije osnovnog toka odrediti će se pouzdanost pojedinačnog rezolucijskog modela pri prikazu Golfske struje. R20 simulacija ( $1/20^\circ$ ) će se pokazati najuspješnijom dok će niskorezolucijski modeli rezultirati nepouzdanim prikazom energetski nerazvijenog cirkulacijskog toka. Također će se uočiti i posebno opisati zanimljive oscilacije u ponašanju simulirane morske struje kao posljedica vrtložnog gibanja fluida. U zaključku, visokorezolucijski modeli su potvrđeni kao adekvatan alat za simuliranje dinamičkih procesa u oceanu i atmosferi na prostorno i vremensko ograničenim domenama.

**Ključne riječi:** Golfska struja, simulacija, rezolucija, NEMO

**Rad sadrži:** 17 stranica, 10 slika, 1 tablicu, 7 literaturnih navoda. Izvornik je na engleskom jeziku.

**Mentor:** izv. prof. dr. sc. Jadranka Šepić

**Neposredni voditelj:** prof. dr. sc. Joakim Kjelsson

**Ocjenjivači:** izv. prof. dr. sc. Jadranka Šepić  
doc. dr. sc. Žarko Kovač  
prof. dr. sc. Mile Dželalija

**Rad prihvaćen:** 24. Studeni 2021.

Rad je pohranjen u Knjižnici Prirodoslovno – matematičkog fakulteta, Sveučilišta u Splitu.

## Basic documentation card

University of Split  
Faculty of Science  
Department of Physics  
Ruđera Boškovića 33, 21000 Split, Croatia

Bachelor thesis

### The impact of model grid resolution on Gulf Stream dynamics in idealised simulations

Roko Topić

University undergraduate study programme Physics

#### Abstract:

The Gulf Stream is one of the biggest and geohistorically most important currents in the world ocean. It emerges as a direct product of mechanical and thermodynamic forcing from the atmosphere and the ocean with the effect of planetary rotation having a major influence on the stream's appearance. Specifically, in this work, the goal will be to compare different simulations of the North Atlantic Ocean using the NEMO ocean model which is based on a set of rules that describe the ocean dynamics - primitive equations. Simulations of an idealised domain, similar to the North Atlantic Ocean, with horizontal resolutions of  $1/2^\circ$ ,  $1/4^\circ$ ,  $1/10^\circ$  and  $1/20^\circ$  are used to reveal how the prescribed parameters and the model resolution affect the behavior of major currents. The location and the kinetic energy of the current will be determined leading to sufficing results when using the R20 ( $1/20^\circ$ ) model as expected from a higher resolution setup while the low resolution runs will display an underdeveloped gyre, inadequate for practical application. Some interesting eddy-consequential perturbations and oscillations in current behavior will also be detected and discussed in this thesis. It is concluded that the general current behavior can be reliably simulated with a high resolution, simplified ocean model in a limited time-space domain.

**Keywords:** Gulf Stream, simulation, resolution, NEMO

**Thesis consists of:** 17 pages, 10 figures, 1 tables, 7 references. Original language: English.

**Supervisor:** izv. prof. dr. sc. Jadranka Šepić

**Leader:** prof. dr. sc. Joakim Kjelsson

**Reviewers:** izv. prof. dr. sc. Jadranka Šepić  
doc. dr. sc. Žarko Kovač  
prof. dr. sc. Mile Dželalija

**Thesis accepted:** November 24, 2021

Thesis is deposited in the library of the Faculty of Science, University of Split.

# Contents

- 1 Introduction . . . . . 1**
- 2 Idealised ocean and NEMO . . . . . 2**
- 3 Results . . . . . 7**
  - 3.1 Equilibration of the model . . . . . 7
  - 3.2 Mean state . . . . . 8
  - 3.3 Gulf Stream variability . . . . . 13
- 4 Discussion . . . . . 15**
- 5 Conclusion . . . . . 16**
- 6 References . . . . . 17**

# 1 Introduction

The Gulf Stream is a warm Atlantic Ocean current that originates in the Gulf of Mexico and stretches to Newfoundland before crossing the Atlantic Ocean. At about 40°N 30°W it splits in two with the northern stream crossing to Northern Europe and the southern stream recirculating off the coast of West Africa [1]. The Gulf Stream transfers great amounts of heated water mass from tropical towards the northern, relatively colder climate zones where it acts as a "warm climate generator" through heat exchange processes with the atmosphere. The behavior and characteristics of the Gulf Stream as well as its impact on the climate of Europe and North America have been the focal points of many research papers [2, 3].

Mesoscale eddies and strong ocean currents such as the Gulf Stream are found at spatial scales of tens of kilometers to several hundred kilometers and timescales of weeks to years [1]. Explicit resolving of these perturbations requires a model with a grid size of at least 25 km, which is roughly equal to 1/4°. Modern computer resources allow global ocean models of up to 1/10° resolution [4], while climate models generally use 1/4° or coarser. High-resolution models offer much detail but are computationally very expensive as the complexity of the problem increases with the grid size reduction. Simulating decades to centuries at a resolution of 1/20° or higher is only possible over limited domains, e.g. the North Atlantic or Mediterranean.

Ocean models can be categorized in three classes: the "non-eddying" models with a grid resolution larger than 50km, which are unable to resolve any mesoscale eddy motion, the "eddy-permitting" models with resolutions varying from 10 to 50 kilometers, which resolve some mesoscale eddys but often underestimate their kinetic energy, and the "eddy-resolving" models with a grid size smaller than 10 km, which fully resolve mesoscale eddys at midlatitudes. Unresolved eddies are typically represented by a harmonic or a bi-harmonic diffusion on tracers and momentum while "non-eddying" models often apply an added diffusion on tracers following the GM scheme [5].

The goal of this thesis is to compare simulations at different horizontal resolutions and describe the resulting differences in the kinetic energy, air-sea fluxes and the position of the associated resolution-dependent gyre. Also, an important objective is to find the optimal resolution model with respect to the computational capacity on an observed timescale with the aim of generalising the used analytic method to more complex models, e.g. the climate system. Consequently, it will be determined if this simplified ocean model is applicable to the North Atlantic basin and if it is sufficient to describe ocean currents such as the Gulf Stream.

## 2 Idealised ocean and NEMO

For the purpose of computing and data analysis, the ocean engine of NEMO (Nucleus for European Modelling of the Ocean), a primitive equation model adapted to regional and global ocean circulation problems, has been used. Prognostic variables are the three-dimensional velocity field,  $(\mathbf{u}, \mathbf{v}, \mathbf{w})$ , the Conservative Temperature,  $T$  and the Absolute Salinity,  $S$ . The model domain is very similar to the one used in Levy et al. [2] with a rectangular basin of 3286 km by 2226 km and a flat bottom at 4200 m depth. The domain is rotated clockwise by  $45^\circ$  to resemble the North Atlantic basin.

The ocean is a fluid that can be described to a good approximation by the primitive equations, i.e. the Navier-Stokes equations along with a nonlinear equation of state which couples the two active tracers (temperature  $T$  and salinity  $S$ ) to the fluid velocity  $\mathbf{U}$  (split into horizontal  $\mathbf{U}_h$  and vertical  $\omega$  component):

$$\frac{\partial \mathbf{U}_h}{\partial t} = -[(\nabla \times \mathbf{U}) \times \mathbf{U} + \frac{1}{2} \nabla(\mathbf{U}^2)]_h - f \mathbf{k} \times \mathbf{U}_h - \frac{1}{\rho_0} \nabla_h p + \mathbf{D}^U + \mathbf{F}^U \quad (2.1)$$

$$\frac{\partial p}{\partial z} = -\rho g \quad (2.2)$$

$$\nabla(\mathbf{U}) = 0 \quad (2.3)$$

$$\frac{\partial T}{\partial t} = -\nabla(T\mathbf{U}) + \mathbf{D}^T + \mathbf{F}^T \quad (2.4)$$

$$\frac{\partial S}{\partial t} = -\nabla(S\mathbf{U}) + \mathbf{D}^S + \mathbf{F}^S \quad (2.5)$$

$$\rho = \rho(S, T, p), \quad (2.6)$$



where  $\nabla$  is the generalised derivative vector operator in  $(x, y, z)$  directions,  $t$  is the time,  $z$  is the vertical coordinate,  $\rho$  is the density,  $\rho_0$  is a reference density,  $p$  the pressure,  $f = 2\Omega\mathbf{k}$  is the Coriolis acceleration (where  $\Omega$  is the Earth's angular velocity vector), and  $\mathbf{g}$  is the gravitational acceleration.  $\mathbf{D}^U$ ,  $\mathbf{D}^T$  and  $\mathbf{D}^S$  are the parameterisations of small-scale physics for momentum, temperature and salinity, and  $\mathbf{F}^U$ ,  $\mathbf{F}^T$  and  $\mathbf{F}^S$  surface forcing terms.

Hydrostatic approximation is given by the second equation. In term (2.6) EOS-80 equation of state [6] is used which prescribes a non linear dependency of density towards salinity and temperature. Mass conservation is provided by equation (2.3). As it is presumed in this simulation that the water is an incompressible fluid, the fluxes in zonal, meridional and vertical direction must cancel out. The heat and salt conservation is given by equations (2.4) and (2.5).

The effects of smaller scale motions (coming from the advective terms in the Navier-Stokes equations) must be represented entirely in terms of large-scale patterns to close the equations. These effects appear in the equations as the divergence of turbulent fluxes (i.e: fluxes associated with the mean correlation of small scale perturbations). It is usually called the subgrid scale physics. It must be emphasized that this is the weakest part of the primitive equations, but also one of the most important for long-term simulations as small scale processes in fine balance the surface input of kinetic energy and heat. For tracers, a second order, or harmonic diffusion is used:

$$\mathbf{D}^T = \nabla(\mathbf{A}^T\nabla T), \quad (2.7)$$

with  $A^T$  being a diffusion coefficient in the given exemplary equation for temperature. When the eddy induced velocity parametrisation (GM) [5] is used, an additional stabilising tracer advection is introduced to the equation (2.7). Fourth order or bi-harmonic diffusion is used to represent the momentum, for example:

$$\mathbf{D}^U = \nabla^2(\mathbf{A}^U\nabla^2\mathbf{U}), \quad (2.8)$$

in case of zonal velocity. This approach is appropriate for implementation in the higher resolution models [3].

$F^U$ ,  $F^T$  and  $F^S$  coefficients are dictated by the physical consideration that a SST anomaly in the ocean interacts with atmospheric fluxes and is modified through this interaction. They are generally formed through following equations:

$$F^U = C^U U_a^2 \quad (2.9)$$

$$F^T = C^T (T - T_a) \quad (2.10)$$

$$F^S = S_r (E - P), \quad (2.11)$$

where  $C^U$  and  $C^T$  are transfer coefficients for momentum and heat,  $S_r$  is a reference salinity,  $U_a$  and  $T_a$  are the wind speed and air temperature,  $E$  is evaporation and  $P$  is precipitation. Hence the direction of sensible heat flux is directed down the temperature gradient across the ocean surface. Air-sea flux coefficients  $F^U$ ,  $F^T$  and  $F^S$  are established by prescribing  $U_a$ ,  $T_a$  and  $E - P$  which are zonally uniform, i.e. only vary in time and latitude. These atmospheric conditions have an imposed seasonal cycle but no inter-annual variability.

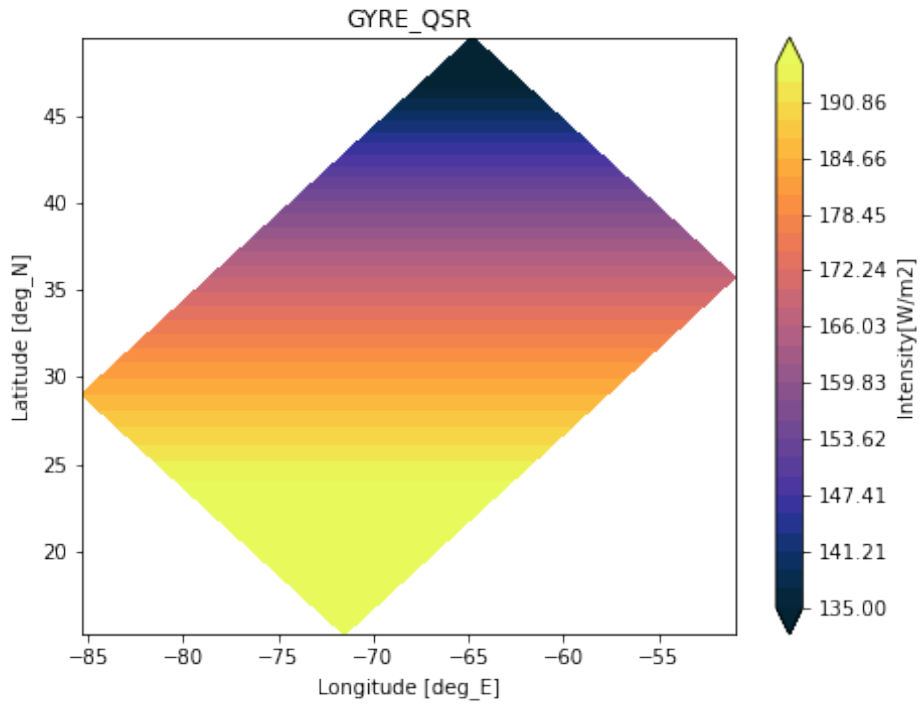


**Figure 1:** Time-averaged solar short wave radiation.

A portion of the net heat flux comes from the solar radiation. Shortwave (solar) heat flux is always directed into the ocean while longwave (terrestrial) heat flux is always directed out of the ocean. Solar heat flux is allowed to penetrate within the water column. The penetrative solar radiation is imposed zonally and grows with latitude as seen from figure 1.

The fresh water flux is prescribed and varies zonally. It is also determined such as, at each time step, the basin-integrated flux is zero. This condition ensures the conservation of salinity. Evaporation decreases with latitude while the precipitation increases as shown in figure 2.

The circulation is forced by analytic profiles of wind and buoyancy fluxes. The applied forcing vary seasonally in a sinusoidal manner between winter and summer extrema. The wind stress is zonal and its curl changes sign at 22°N and 36°N. All simulations use wind forcing, heat fluxes and freshwater fluxes identical to Levy et al [2].

This thesis will be handling four models with horizontal resolutions R2 (1/2°), R4 (1/4°), R10 (1/10°) and R20 (1/20°). Detailed description of each model's technical parameterization is given in table 1.

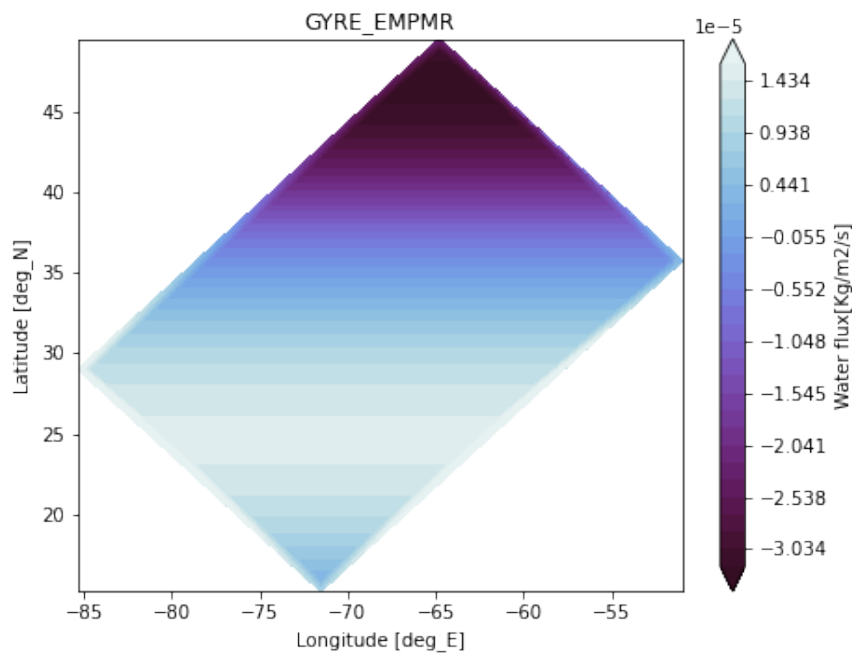


**Figure 2:** Time-averaged freshwater flux,  $E - P$ .

Parameters	Resolution			
	R2	R4	R10	R20
Grid size	53km	26.5km	10.6km	5.3km
Problem size	62 x 42 x 31	122 x 82 x 31	302 x 202 x 31	602 x 402 x 31
Node hours	0.09	0.3	3.2	24
Time step	1800s	1440s	600s	300s
Eddy viscosity	$-72 \times 10^{10} \text{m}^4/\text{s}$	$-2.25 \times 10^{10} \text{m}^4/\text{s}$	$-2.16 \times 10^{10} \text{m}^4/\text{s}$	$-0.27 \times 10^{10} \text{m}^4/\text{s}$
Eddy diffusivity	$600 \text{m}^2/\text{s}$	$300 \text{m}^2/\text{s}$	$120 \text{m}^2/\text{s}$	$60 \text{m}^2/\text{s}$
GM scheme	applied	N/A	N/A	N/A

**Table 1:** *Properties of individual resolution models.*

### 3 Results

#### 3.1 Equilibration of the model

The experiments were run over 40 years, which satisfied the time required to equilibrate the mean circulation and to stabilise the model's energy profile. The stabilization of gyre circulation is shown by a vertically integrated KE (kinetic energy) timeseries in figure 3. Model starts with zero velocity values and no horizontal gradients. First few years of simulation can be neglected as energy influx and energy dissipation aren't balanced in this time period. After the stabilisation, it can be noted that the R20 model poses the highest KE at around 40TJ with decreasing trend towards R2 model which is set to  $\sim 4$ TJ. The overall kinetic energy displays oscillations in yearly periods which are more pronounced in higher resolution runs.

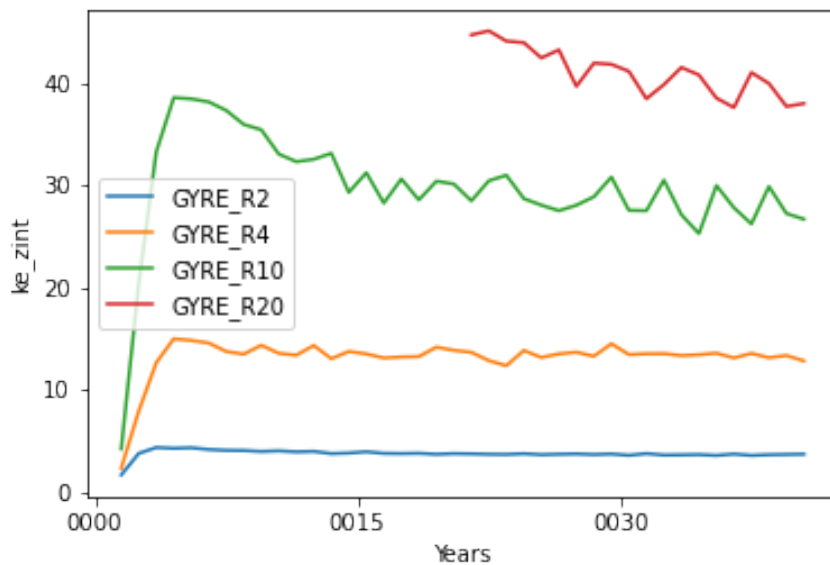


**Figure 3:** Vertically integrated kinetic energy of each resolution model.

### 3.2 Mean state

As a consequence of periodical external wind forcing, sea surface level pressure, buoyancy flux and internal features of the ocean such as an inhomogeneous density and temperature profile, an uneven mean SSH (Sea surface height) can be observed over the domain. For resolutions R10 4c) and R20 4d) the sea surface has its mean maximum values at 29°N and 83°W with steep latitudinal decrease towards north along the 30°N parallel. Also the SSH gradient is consistently weakening eastwards across this parallel until reaching the domain limit. In the case of R2 4a) and R4 4b) the SSH has a similar maxima location but with gradient being the strongest alongside the northwestern gridline with eastwards gradient persisting only until 65°W.

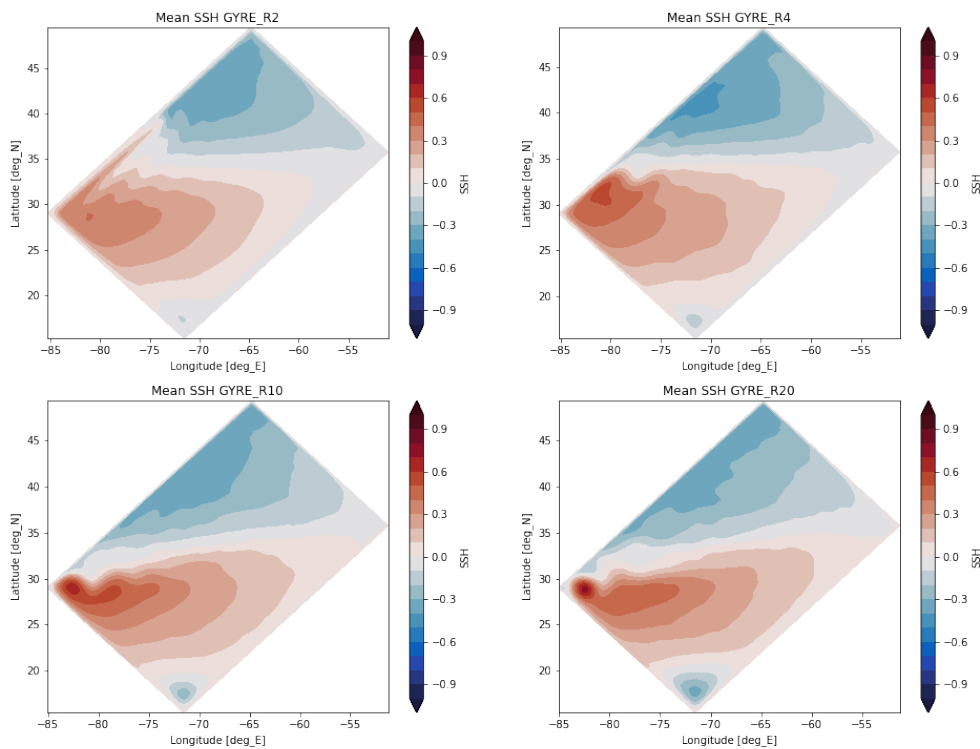


**Figure 4:** Mean surface height. a)R2(top-left), b)R4(top-right), c)R10(bottom-left), d)R20(bottom-right).

SSH distribution indicates the fluid movement arrangement as the process of diffusion compels the water mass to follow the SSH gradient, with higher velocities along the steeper changes of the surface height. Mean ocean surface kinetic energy corresponds to this assessment as shown in figure 5. The values of kinetic energy are represented in  $m^2/s^2$  (per unit of mass). The gyre, which can be defined along the high kinetic energy spread, doesn't separate from the northwestern gridline in R2 representation fig 5a). R4 model 4b) displays a very weak longitudinal dispersion of kinetic energy at latitudes of  $33^\circ\text{N}$  reaching out only to  $77^\circ\text{W}$ . R10 5c) and especially R20 5d) show a eastwards developing gyre with higher kinetic energy spread over the domain.

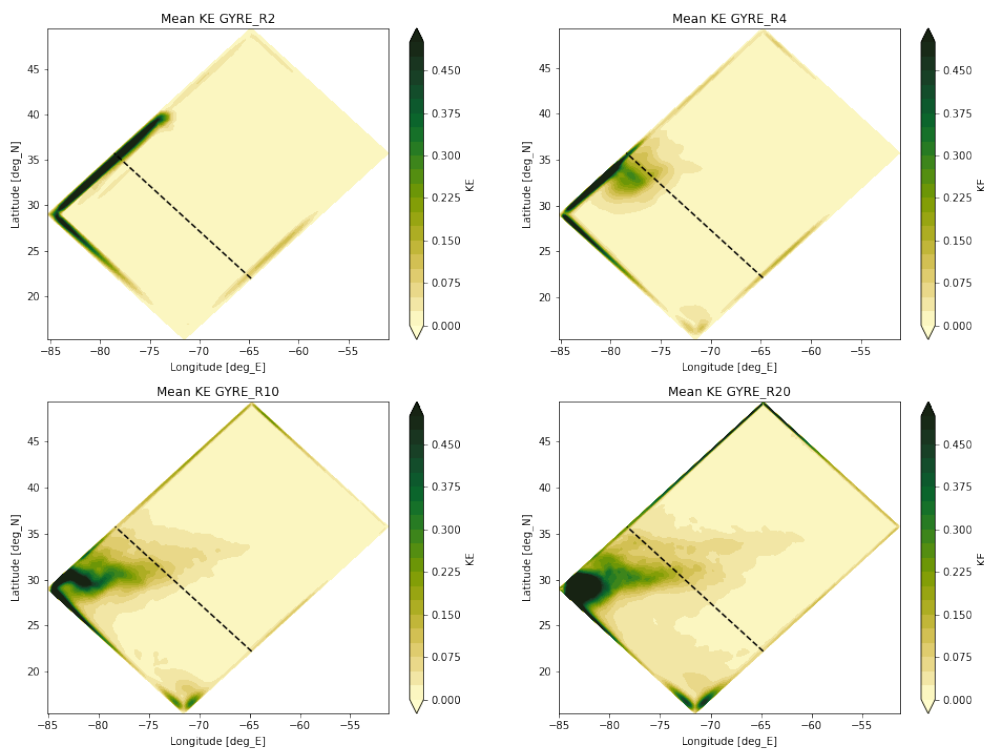


**Figure 5:** Mean surface kinetic energy. a)R2(top-left), b)R4(top-right), c)R10(bottom-left), d)R20(bottom-right).

Mean SST (Sea surface temperature) varies with latitude similar to figure 1 as it is heavily influenced by the short wave solar radiation's heat influx. Despite of this, the turbulent ocean surface layer alters the SST mean distribution as shown in figure 6. R2 model 6a) supports a high temperature deformation along the northwestern grid up to  $40^{\circ}\text{N}$ , which is also visible from a R4 run 6b) but only reaching  $33^{\circ}\text{N}$ . Higher resolution simulations show a more smooth transition between latitudinal temperature zones with temperatures higher than  $20^{\circ}\text{C}$  reaching  $30^{\circ}\text{N}$ .

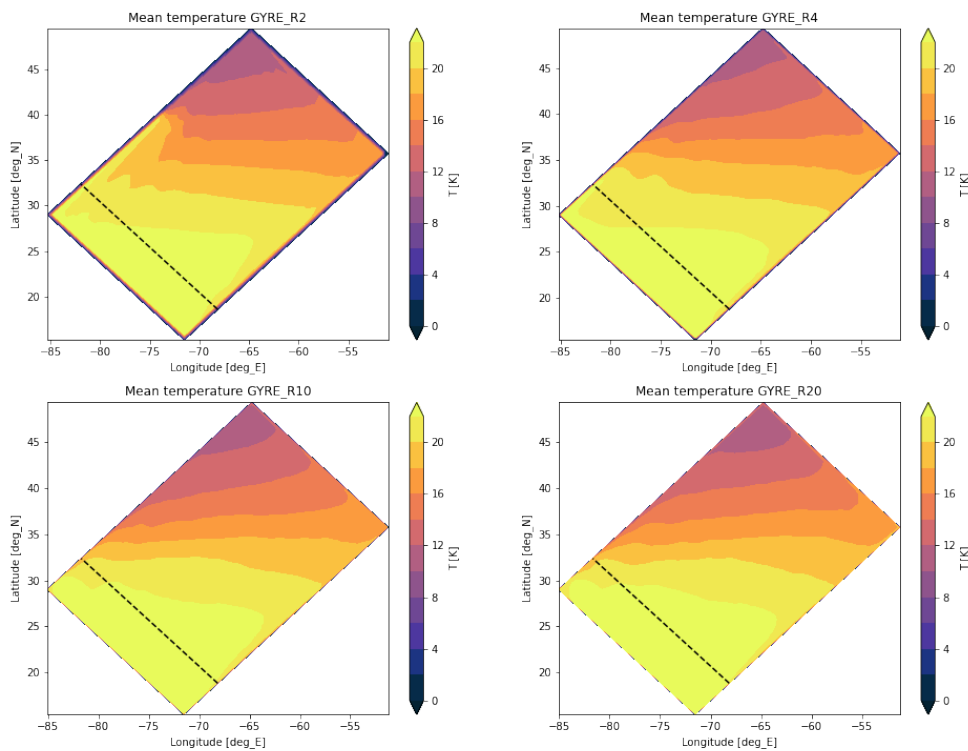


**Figure 6:** Mean surface temperature. a)R2(top-left), b)R4(top-right), c)R10(bottom-left), d)R20(bottom-right).



Depth profile of temperature separates the ocean into vertically isothermal layers. At depths below 1200 m water temperature changes are negligible. In R2 and R4 20°C temperature reaches the depths of 100 meters which is only half of the maximum depth that the same temperature layers reach for R10 and R20 runs as seen from figure 7 which also shows the cross section used to analyse the temperature. Temperature layer maximum depth is set at latitudes of 32°N, not separating from the domain gridline, in case of R2 7a) and R4 7b) simulations. This feature changes for R10 7c) with layer depth set at 29° of latitude and 28° of latitude for R20 7d) without steep temperature gradient as compared to R2 7a).

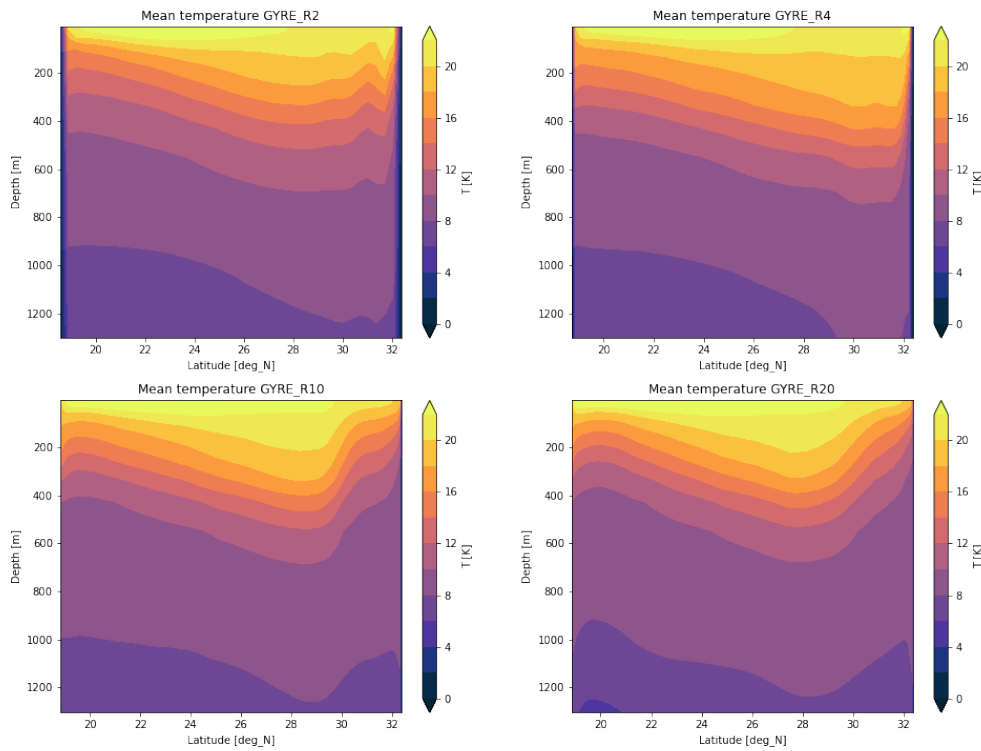


**Figure 7:** *Temperature depth profile. a)R2(top-left), b)R4(top-right), c)R10(bottom-left), d)R20(bottom-right).*

Atmosphere and the ocean exchange heat through the ocean’s surface. This heat flux can be directed upwards or downwards, depending on temperature differences among the two systems. R2 simulation 8a) displays highest upwards outgoing values of heat along the northwestern gridline with values decreasing with distance to this basin boundary. R4 model 8b) has a detaching "streamline" of hot water at 33°of latitude which doesn’t go further than 75°W. "Streamline" in R10 8c) and R20 8d) models is well developed westwards, stemming from the origin point of 30°N and 85°W, and transferring notable amount of heat in areas ranging all the way up to 64°W.

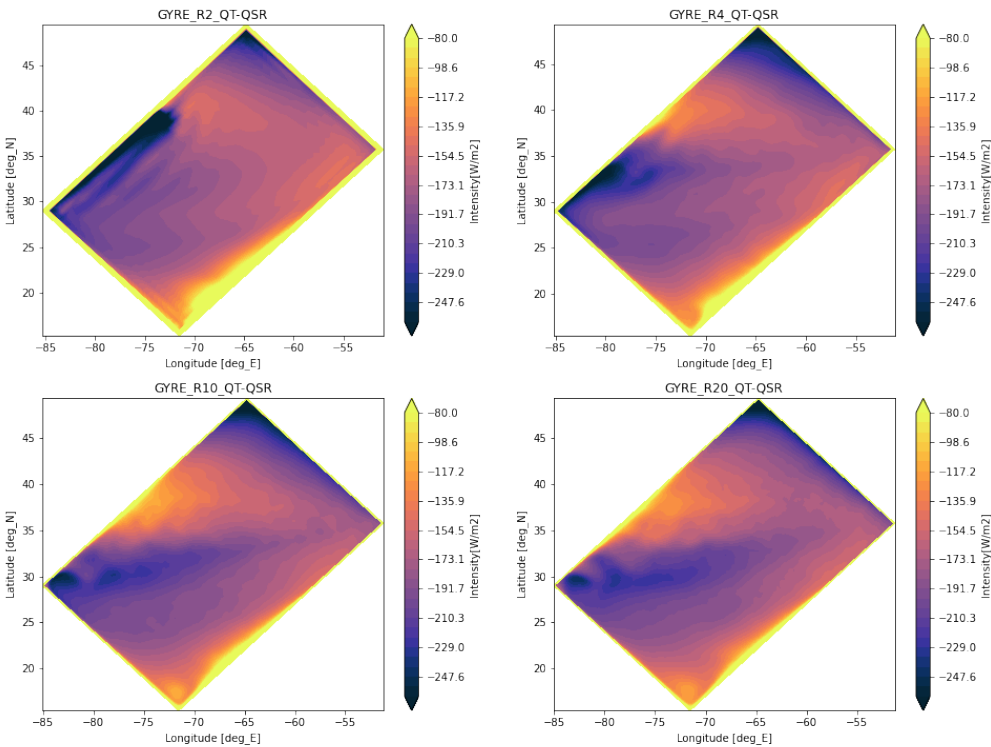


**Figure 8:** Total non-solar heat flux between the sea and the atmosphere, a)R2(top-left) b)R4(top-right) c)R10(bottom-left) d)R20(bottom-right).

### 3.3 Gulf Stream variability

Surface kinetic energy maximum values at a cross section marked in figure 5 during the last 10 years of simulation are portrayed in a timeseries graph given by figure 9. R2 run is characterised by a relatively time-consistent maximum value with negligible deviations in interannual periods. The kinetic energy maximum observed in this run is notably high at around  $0.95 \text{ m}^2/\text{s}^2$ . R4 model portrays a timeseries function with values ranging from 0.2 to  $0.65 \text{ m}^2/\text{s}^2$ . This function reaches its maximum two times during the evaluation period with 6 years difference between these two events. R10 and R20 runs have a surface kinetic energy maximum set at around  $0.2 \text{ m}^2/\text{s}^2$  with interannual deviations reaching values of  $0.1 \text{ m}^2/\text{s}^2$ .

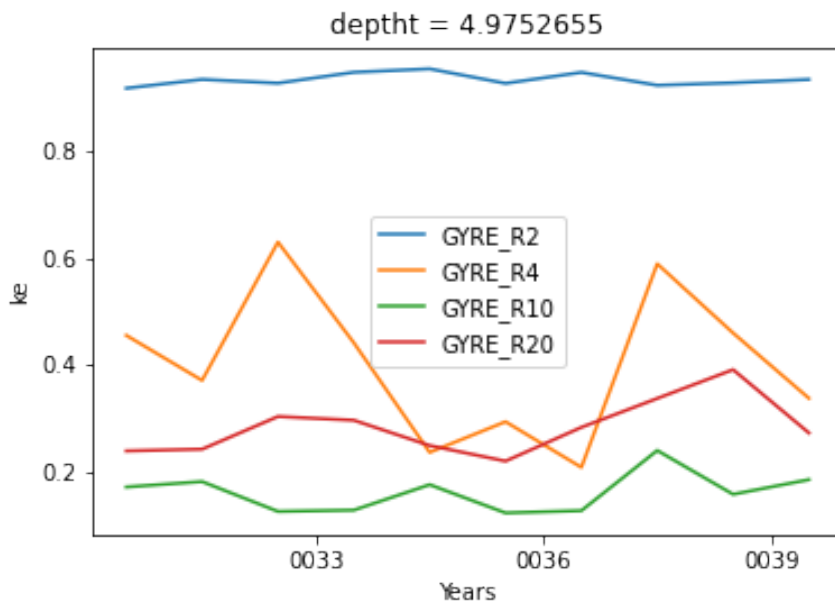


**Figure 9:** Maximal surface kinetic energy at a cross section.

The latitudinal position of the maximum is represented by a timeseries 10. For R2 model surface KE maximum doesn't relocate throughout time. It is constantly placed at a latitude close to  $35^\circ$ . North-South oscillations can be observed for other runs which are particularly emphasised in R10 and R20 runs. R4 simulation has a maximum with varying position around  $33^\circ\text{N}$ . As for R10 and R20 models, the latitudinal annual change reaches over  $3^\circ$  in a meridional direction with R20 model's maximum going as south as  $29^\circ\text{N}$ .

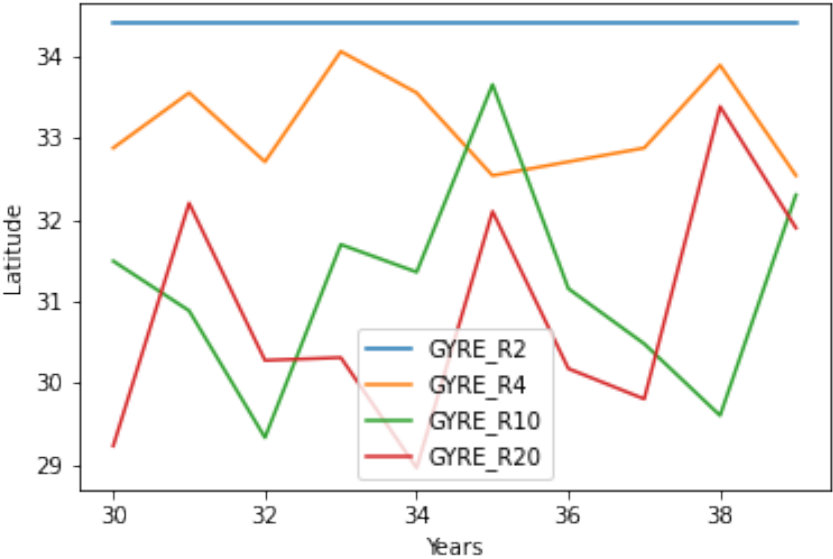


**Figure 10:** Latitudinal position of the maximal surface kinetic energy at a cross section.

## 4 Discussion

The difference between gyre representations of the implemented resolution models corresponds to "inter-resolution" changes noted in Levy et al [2]. As seen in figure 3 the overall mean kinetic energy in resolution runs decreases with increase in resolution. This can be attributed to higher viscosity coefficient for low resolution models shown in table 1 which increases energy dissipation. Consequently, as suggested by figure 5, R2 model's surface energy distribution is constrained to the northwestern coastline with R4 showing only a minimal zonal improvement at 33°N. R10 and R20 runs represent a more faithful display of the Gulf Stream with a band of kinetic energy extending eastward into the basin interior. This statement is supported by the latitudinal temperature shifts at moderate depths for R10 and R20 simulations shown in figure 7. This temperature anomaly can be interpreted as a relatively warmer flow of water which is separated from the coastline and crosses the ocean model at 30°N. The consequential heat exchange along this flow is visualised in the heat flux figure 8 and can be used to describe the Gulf Stream's heating effect on North America and Europe. Comparative research between "eddy-permitting" and "eddy-resolving" models has been documented in the work of Kjellsson/Zanna [3]. They find that due to discrepancies in the effect of wind forcing, horizontal viscosity, potential to kinetic energy, conversion, and nonlinear interactions on the kinetic energy budget the energy cascades of these two models will differ significantly. This can be applied to R4 and R10/R20 runs studied here. Suggestion for improving the "eddy-permitting" model is to parameterise the effect of mesoscale eddies by enhancing the potential to kinetic energy conversion [3].

As kinetic energy is defined by the fluid velocity, the maximum surface KE value and its position represent the latitudinal and longitudinal position of the fastest moving gyre's stream section. The R2 model results in a high KE stream at a constant latitude of 35°. In contrary, R4 run shows a decrease in KE with oscillating values and north-west shift of latitudinal position. At given cross section of the basin, the R20 model has higher KE then the R10 model with both displaying a interannual latitudinal deviations of approximately 4°. This periodical change of position is documented and analysed in the work of Joyce et al.[7] which correlates this behavior to the phase shift between external forcing and ocean's potential vorticity. They find the Gulf Stream path variability to be at least 2° of latitude. It is important to note that the tracking method used in the work of Joyce et al.[7] relies on observing the 15°C isoline at 200m depth which clearly differs from the method used in this thesis. Also the interannually identical external forcing and a flat bottom basin prescribed here have an effect on the difference in the resulting shift.

From the results it is clear that higher resolution runs (R10 and R20) display a reliable Gulf Stream simulation, meaning that this method of the ocean's behaviour modeling can be expanded from simplified ocean models, such as this one, to more complex ones. It can be applied to topographically rigid basins, i.e. the Mediterranean sea, the North Pacific Ocean or the North Atlantic Ocean with a complex bottom, as the ocean floor topography negligibly affects the results with most of the energy and heat exchange processes happening in the ocean's upper layers. When adding a dynamic, spatially distributed ice layer over the ocean's surface, it is to be expected that the air-sea heat flux will be severely modified as the solar shortwave radiation reaching the ocean will be dependent on the ice coverage. This would be a major factor when applying this model to sea masses near the Earth's poles, i.e. the Arctic and Antarctic circle. Applying an annually alternating external forcing could result in a higher main current spatial variability but it would be hard to prove this statement as it is out of scope of this thesis. The remote effects of nearby oceans should also be considered as here they are replaced by non-penetrable solid boundaries.

## **5 Conclusion**

It has been proven that with increase in model resolution the simulated gyre more reliably encaptures the Gulf Stream's behavior. The downside of this precision improvement is the computing time and resources needed to support the high resolution simulations which is due to their relatively big problem size and node hours length as shown in table 1. Optimally, the R10 method presents itself as a best choice in terms of time preservation and result faithfulness. Although, it should be noted that some physics such as topographic effects or the contribution of water mass formation in marginal seas are not taken into account in our idealized experiments. Despite this, the results are descriptively reliable and could be well implemented into a more complex climate model.

## 6 References

### Bibliography

- [1] Lynne D. Talley, George L. Pickard, William J. Emery, James H. Swift. *Descriptive Physical Oceanography*,(2011). <https://doi.org/10.1016/C2009-0-24322-4>.
- [2] Marina Lévy, Patrice Klein, Anne-Marie Tréguier, Doroteaciro Iovino, Gurvan Madec, et al. *Modifications of gyre circulation by sub-mesoscale physics*. *Ocean Modelling*, Elsevier, 2010, 34 (1-2), pp.1-15. <https://doi.org/10.1016/j.ocemod.2010.04.001>.
- [3] Kjellsson, Joakim and Zanna, Laure. *The Impact of Horizontal Resolution on Energy Transfers in Global Ocean Models*. *Fluids*, 2017, 2(3), 45. <https://www.mdpi.com/2311-5521/2/3/45>.
- [4] Stephen M. Griffies et al.. *Impacts on Ocean Heat from Transient Mesoscale Eddies in a Hierarchy of Climate Models* . *Journal of Climate*, 2015, Vol 28 (3), pp.952–977. <https://doi.org/10.1175/JCLI-D-14-00353.1>.
- [5] Peter R.Gent. *The Gent–McWilliams parameterization: 20/20 hindsight*. *Ocean Modelling*, (2011), 39 (1–2), pp.2-9. <https://doi.org/10.1016/j.ocemod.2010.08.002>.
- [6] Trevor J. McDougall. *Neutral Surfaces*. *Journal of Physical Oceanography*, (1987), 17 (11). [https://doi.org/10.1175/1520-0485\(1987\)017<1950:NS>2.0.CO;2](https://doi.org/10.1175/1520-0485(1987)017<1950:NS>2.0.CO;2).
- [7] Terrence M. Joyce, Clara Deser, Michael A. Spall. *The Relation between Decadal Variability of Subtropical Mode Water and the North Atlantic Oscillation* . *Journal of Climate*, (2000), 13 (14). [https://doi.org/10.1175/1520-0442\(2000\)013<2550:TRBDVO>2.0.CO;2](https://doi.org/10.1175/1520-0442(2000)013<2550:TRBDVO>2.0.CO;2).